ACCST Research Journal **ISSN 0972-7779**
Volume - XXI, No. 1, January 2023
Refereed and Peer-Reviewed Quarterly Journal
Journal website : www.internationaljournalsiwan.com

Monitoring Land Use / Land Cover Changes and Land Surface Temperature of Dewal Block, Chamoli District, Garhwal Himalaya from 1990 to 2022

by **Surajmal Junawa,** *Research Scholar,*
Department of Geography,
Delhi School of Economics, University of Delhi - 110007
E-mail: suraj1998jat@gmail.com

Abstract:

Land use and land cover change (LULCC) is the alteration of the terrestrial surface of the earth by human interference. LULCC is affected by social economic and natural activities. RS and GIS have capabilities for land change detection, land planning, hazard mapping, etc. The objective of this study is to monitor the land use/ land change and Land Surface temperature (LST) from 1990 to 2022 with help of remote sensing (RM) and Geographic Information system (GIS). The results indicate that in Dewal for the period between 1990 to 2022, the area under vegetation, which occupied 433.14 km^2 in 1990, decreased to 412.84 km^2, accounting for a decrease of 4.68%, indicating a high loss of vegetation in these 32 years. Between 1990 and 2022, snow cover decreased by 34.77% and in terms of 36.09 km^2 in the last 32 years. The snow cover and vegetation land cover are converting into barren land. LST is also increased significantly near 9.73°C in the last 32 years.

Keywords: Land use and Land cover; Land surface temperature; Remote sensing and Accuracy assessment

Introduction:

Land use and land cover change (LULCC) is the changeable terrestrial earth surface by human interference (Lu et al. 2004). Its have impact on climate, soil, ecosystem services, biodiversity, etc. and it has become a serious environmental issue in recent times (Hailemariam et al. 2016). LULCC is affected by social economic factors and man-nature interaction. Uncontrolled population growth rate increases to the encroachment of farming and grazing on the earth's surface. Bio geochemical cycle, river channels, and people's livelihoods are affected by changing condition of land cover and its composition (Samie et al. 2020). Understanding the Spatio-temporal monitoring of LULCC at regional, and national is important to synthesize knowledge on the relationship between humans and nature (Kapur et al. 2022; Verburg et al. 2015). Many techniques are used for the calculation of land cover change detection and LST.

In the literature, RS and GIS have capabilities for land change detection, land planning, hazard mapping, etc. (Kumar et al. 2018; Pal and Ziaul 2017; Rahaman et al. 2020). LULCC technique helps to ensure sustainable development and increase knowledge of changing environment dynamics. The technique is classified into supervised and unsupervised classification (Zewdie et al. 2015). The mountain ecosystem is complex to understand because it passes for changes in the landscape. The ecosystem based on Hindu Kush Karakoram and Himalayan (HKH) region is determined by rapid urbanization, population, industrial development, climate change, and also by natural activities such as landslides, earthquakes, snow melting, etc. (Hailemariam et al. 2016; Lu et al. 2004; Samie et al. 2020; Verburg et al. 2015; Wang et al. 2020). The goal of this research is to monitor the land use / land change and LST from 1990 to 2022 help of remote sensing (RM) and Geographic Information system (GIS).

Study Area:

Dewal block is located in the Chamoli district of Uttarakhand. It is situated between 30° 3' 39.9594" E and 79° 34' 37.92" N and altitude between 1201m to 6403m. Dewal is the part of Pinder River sub-basin. This region is covered by evergreen forests with coniferous plant species. This region is geologically active and comprised of Gneiss, granite, and schist as foundational rocks. Mostly rain is gained in the monsoon session and also the climate is affected by western disturbance. The

primary base of the economy of dewal is agriculture and livestock rearing. Migration is the most common phenomenon in the region due to physiographical and natural challenges.

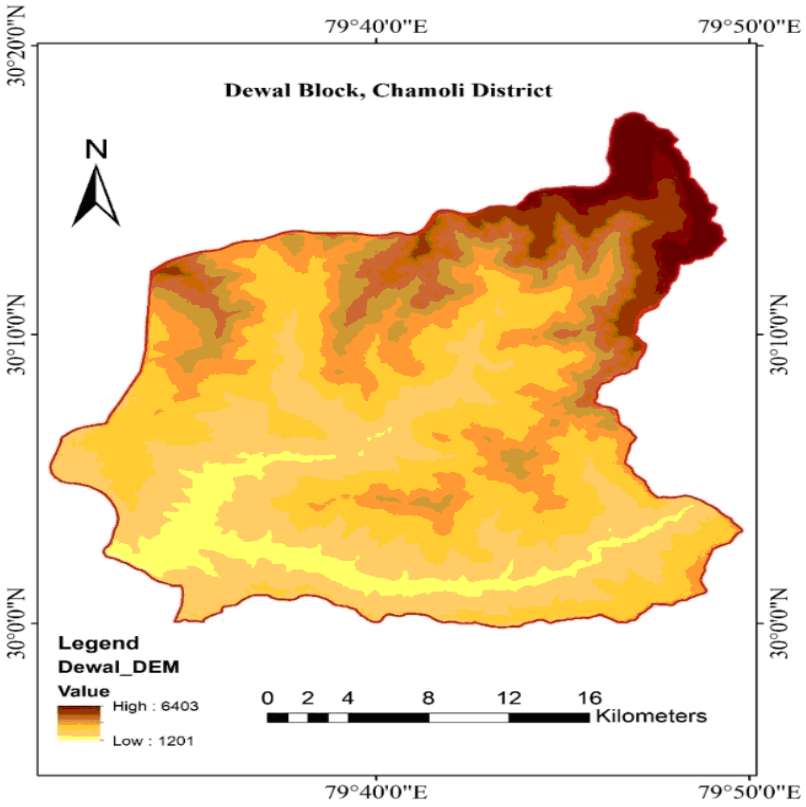

Figure 1: Map of study area

Materials:

Multi-temporal 5, Thematic mapper 4-5(TM) and Lands at 8 OLI-TIRS imageries of March 1990 and March 2022 respectively is used for mapping LULC classes and LST of Dewal Block from 1990 to 2022 (Table 1, Figure 2). The main application of both sensors 9 (TM and OLI- TIRS) is in the areas of coastal, and inland water resources, forest, agriculture and LULC monitoring and mapping. Cartosat DEM is used in this research. Landsat satellite imageries ere collected from USGS (https://earthexplorer.usgs.gov/).

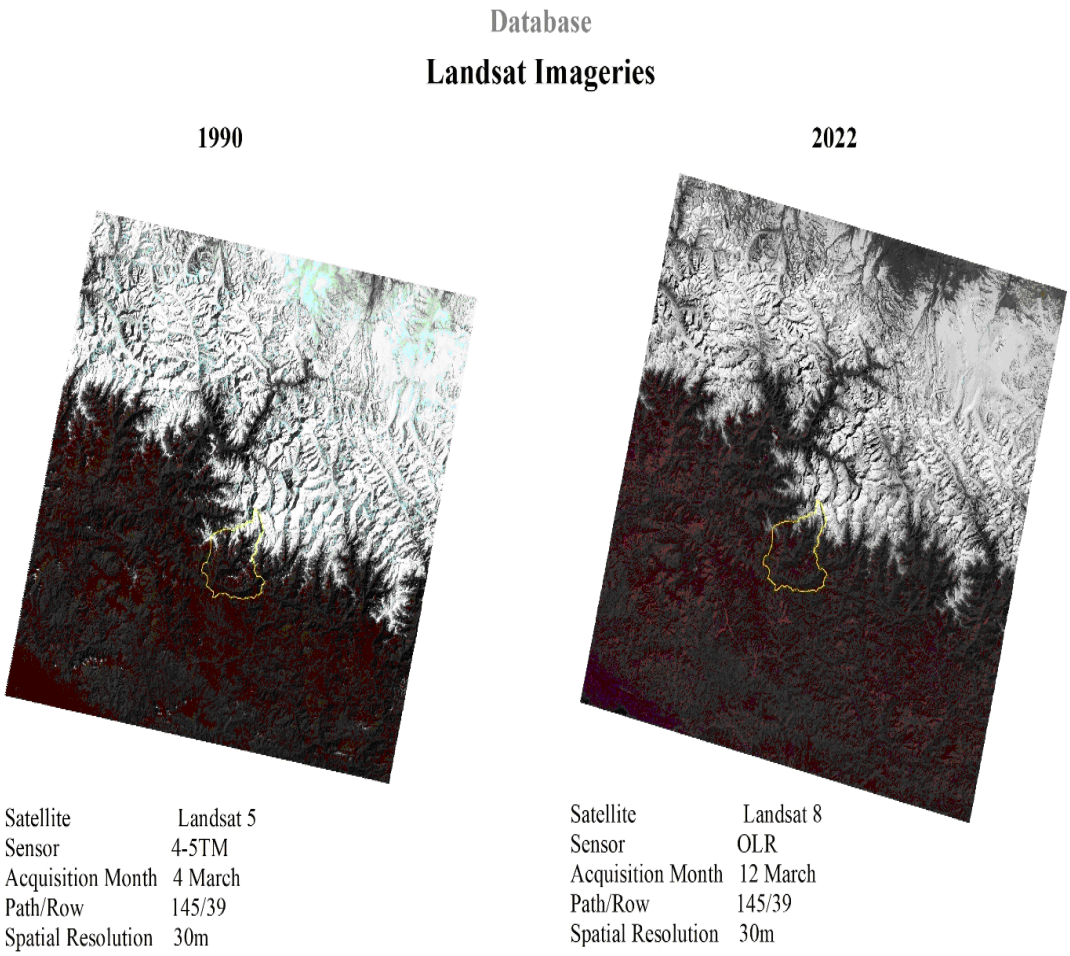

Figure 2: Map of Landsat Imagery

Year	Satellite	Sensor	Acquisition Month	Path/Row	Spatial Resolution
1990	Landsat 5	4-5TM	March	145/39	30m
2022	Landsat 8	OLI-TIRS	March	145/39	30m

Table 1: Details of Landsat imagery used in this research

Methodology:

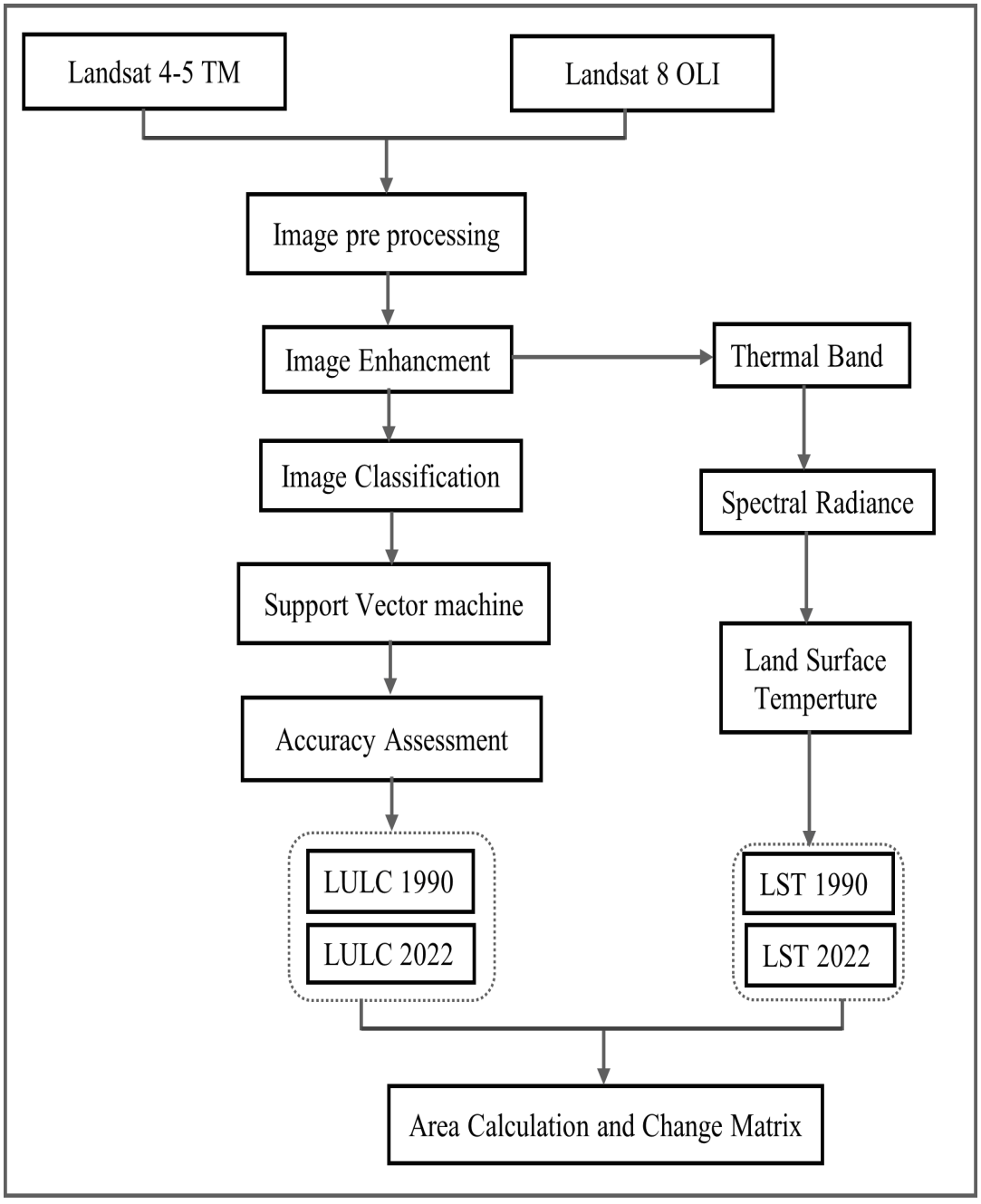

Figure 3: Flowchart of methodology for this study

LULC Classification:

Four major LULC classes were chosen for mapping the study area viz; snow cover, vegetation, barren land, and water bodies. After deciding technique is employed, which is supervised classification. For each desired output class of LULC from imagery, 120 to 150 training samples were selected. To verify the signatures selected for classification all the features of the study area were cross-checked with Google Earth Images.

LULC Accuracy Assessment:

Kappa accuracy assessment techniques were selected to assess the accuracy of classified maps of both 1990 and 2022, which are widely used in various studies. For the classified image of 1990, overall classification accuracy is found to be 81.23% with 0.75 overall kappa statistics whereas, for the classified image of 2022, the overall classification accuracy is found to be 86.72% with the overall kappa statistics of 0.81. Table 3 shows the error matrix and individual producers and users' accuracy of all the classes for image 1990 respectively and similarly Table 2 for the image of 2022.

Year	**1990**		**2022**	
LULC	U/A (%)	P/A (%)	U/A (%)	P/A (%)
Snow cover	100	73.52	95.45	79.25
Vegetation	85	95.65	90	78.66
Barren land	63	88.10	85.32	91.15
Water Body	72	70.12	81.23	83.12
Overall Accuracy	**81.23**		**86.72**	
Kappa Coefficient	**0.75**		**0.81**	

Table 2: Accuracy Assessment matrix of 1990 and 2022

LST Extraction:

LST retrieval from satellite images

Firsty step is to convert the DN number into the radiance.

If an object's temperature is greater than absolute zero, it will release thermal and electromagnetic energy (K). This theory allows for the conversion of the signals from the thermal sensors to at-sensor radiance. The following equation is used to compute the spectral radiance ($L\lambda$).

$$L\lambda = \text{“}gain\text{”} \times QCAL + \text{“}offset\text{”} \tag{1}$$

where DN refers digital value associated with a particular pixel, gain is denotes the slope of the radiance/DN conversion, and bias is the curve of the function. Other names for this are:

$$L\lambda = L_{\min_\lambda} + \left[\frac{\left(L_{\max_\lambda} - L_{\min_\lambda}\right)}{\left(Q_{CAL\max} - Q_{CAL\min}\right)} \times Q_{CAL} \right] \tag{2}$$

where Q_{CAL} is Digital number and $Q_{CAL_{\text{MAX}}}$ is 255.

Digital values 0 and 255 are spectral radiance for band 6, respectively, are L_{MIN_λ} and L_{MAX_λ}. The calculate to 3.2 $\text{W.m}^{-2}\text{sr}$ and 12.65 $\text{W.m}^{-2}\text{sr}$.

$$L\lambda = 0.037059 \times DN + 3.2 \tag{3}$$

Step 2: Spectral radiance ($L\lambda$) to temperatures brightness (TB).

Emissivity (ε) has been added to radiant temperatures based on land cover types. Particularly, vegetated areas scored 0.95, whereas non-vegetated areas scored 0.92(Nichol 1994). The emissivity adjusted surface temperature was calculated in accordance with (Artis et al. 1982)

$$TB = \frac{K_2}{\ln\left(\frac{K_1}{L_\lambda} + 1\right)} \tag{4}$$

Where, brightness temperature is TB and spectral radiance is $L\lambda$ in $\text{W.m}^{-2}\text{sr.}\mu\text{m}^{-1}$. Two calibration parameters used before launch are K_1 and $K_2 = K_1$ and K_2. These compute to 1282.71 K and 666.09 $\text{W.m}^{-2}\text{.sr}^{-1}\text{.}\mu\text{m}$ respectively, for the Landsat 7 ETM + 6.2 band.

Step 3: Retrieval of land surface temperature (LST) :

The temperatures that were determined above are in reference to a black object. Corrections for spectral emissivity (ε) are therefore required. These can be done based on the kind of land cover (Snyder et al. 1998) or by calculating equivalent emissivity values for each pixel from the Normalized Differences Vegetation Index (NDVI) data. The emissivity modified land surface temperature (LST) was calculated using (Artis and Carnahan 1982) formula.

$$(Pv)\varepsilon = 0.004 * Pv + 0.986 \tag{5}$$

$$LST = \frac{TB}{[1+\{(\lambda \times TB/\rho) \times \ln\varepsilon\}]} \tag{6}$$

$$Pv = \left(\frac{NDVI_{jr} - NDVI_{MIN}}{NDVI_{MAX} + NDVI_{MIN}} \right)^2 \tag{7}$$

Step 4: Conversion of surface temperature from Kelvin to degrees Celsius:

For better understanding, the LST unit was exchange to degrees Celsius through this formula 0 °C = 273.15 K.

Result and Discussion:

Figure 4: LULC of Dewal Block in 1990 and 2022.

The results indicate that in 1990, vegetation (433.14 km^2) was the widest land cover in the Dewal block which accounts for 71.94% of the total area followed by snow cover (103.78 km^2) 17.24%, barren land (64.70 km^2) 10.75% and water body (0.47 km^2) 0.08% (Figure 3 and 4, Table 3). The water body includes River Pindar and River Kali along with her tributaries. Whereas, in 2022, the forest is the largest land cover too with an area of 412.84 km^2 contributing 68.57% followed by barren land (120 km^2) 19.93%, snow cover (67.69 km^2) 11.24%, and water body (1.56 km^2) 0.26%.

LULC Class	1990		2022	
	Area (km^2)	(%)	Area (km^2)	(%)
Snow Cover	103.78	17.24	67.69	11.24
Vegetation	433.14	71.94	412.84	68.57
Barren Land	64.70	10.75	120.00	19.93
Water Body	0.47	0.08	1.56	0.26
Total	602.08		602.08	

Table 3: Land use Land cover area distribution between 1990 and 2022.

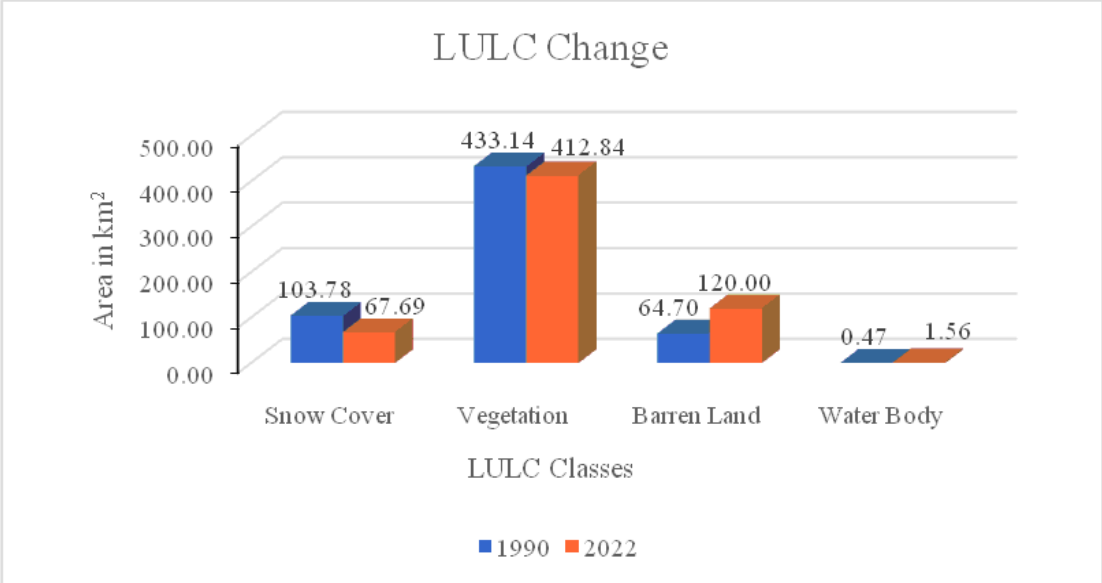

Figure 5: Comparison between LULC classes of 1990 and 2022.

The result shows that in Dewal for the period between 1990 to 2022, the area under vegetation, which occupied 433.14 km^2 in 1990, decreased to 412.84 km^2, accounting for a decrease of 4.68%, indicating a high loss of vegetation in these 32 years. Between 1990 and 2022, snow cover decreased by 34.77% and in terms of 36.09 km^2 in the last 32 years (Kumar et al. 2016). Snow cover and vegetation land convert into barren land that we can see in figure 5. And water bodies' area remains almost same positions.

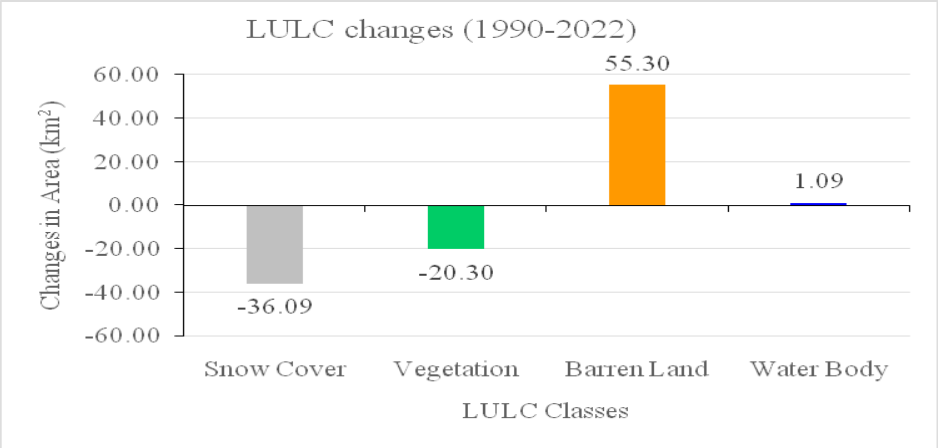

Figure 6: Diagrammatic illustration of LULC of Dewal block

Estimation of LST :

In this study, we used Landsat thermal band to estimate the magnitude of LST in the Dewal Block. Two Landsat images were taken i.e., Landsat 4-5 TM on 3 March 1990 and Landsat 8 OLI on 12 March 2022. We can see that LST increased significantly in the study area. The LST mapping was divided into five classes (Figure 6).

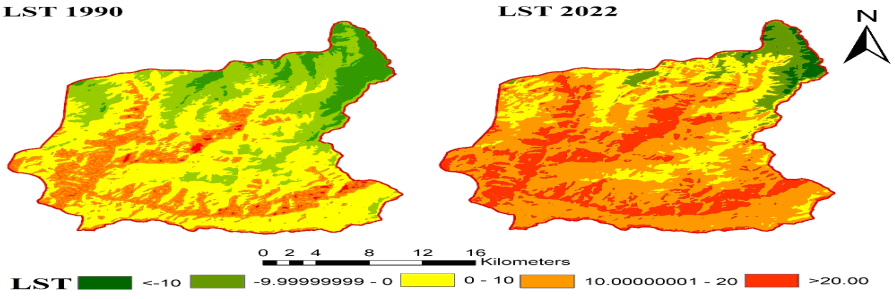

Figure 7 : Map of Dewal LST (°C) for 1990 and 2022.

The mean LST was observed at 3.43°C in 1990 and 13.16°C in 2022 (Table 4). It is near to 9.73°C increase because barren land increased by 85.47% from 1990 to 2022.

LST	1990	2022
Maximum	24.97°C	37.05°C
Minimum	-28.13°C	-24.13°C
Mean	3.43°C	13.16°C

Table 4: LST change matrix of Dewal Block

Conclusion:

This study examines information about Spatio-temporal LULCC in the Dewal block in the last 32 years from 1990 to 2022 with help of remote sensing (RM) and geographical information system (GIS). The research based on Landsat imageries time series over 2 times 1990 and 2022 revealed that snow cover change is significate over the last 32 years. It's almost near to 36.09 km^2 and vegetation is also decreased. And LST are also increased significantly in last 32 years near to 9.73°C in dewal block. Decreasing vegetation and increasing LST have an impact on local community livelihood and sustainable development. The snow cover and vegetation land cover are converting into barren land. The limitation of this study is high satellite image resolution was not available due to the border area.

References:

Artis, David A., and Walter H. Carnahan. (1982): "Survey of Emissivity Variability in Thermography of Urban Areas." 329:313-29.

Hailemariam, Sisay Nune, Teshome Soromessa, and Demel Teketay. (2016): "Land Use and Land Cover Change in the Bale Mountain Eco-Region of Ethiopia during 1985 to 2015." *Land* 5(4). doi: 10.3390/land5040041.

Kapur, Astha Smarth, Pankaj Kumar, G. Areendran, and Krishna Raj. (2022): "The Magnitude of Transformation in Land Use Land Cover of Kalyan-Dombivli, Smart City BT - Remote Sensing and Geographic Information Systems for Policy Decision Support." Pp. 299-316 in, edited by R.B. Singh, M. Kumar, and D.K. Tripathi. Singapore: Springer Nature Singapore.

Kumar, Manish, and Pankaj Kumar. (2016): "Snow Cover Dynamics and Geohazards: A Case Study of Bhilangna Watershed, Uttarakhand Himalaya, India." *Geoenvironmental Disasters* 3(1):2. doi: 10.1186/s40677-016-0035-z.

Kumar, Pankaj, Arif Husain, Ram Babu Singh, and Manish Kumar. (2018): "Impact of Land Cover Change on Land Surface Temperature: A Case Study of Spiti Valley." *Journal of Mountain Science* 15(8):1658-70. doi: 10.1007/s11629-018-4902-9.

Lu, D., P. Mausel, E. Brondízio, and E. Moran. (2004): "Change Detection Techniques." *International Journal of Remote Sensing* 25(12):2365-2401. doi: 10.1080/0143116031000139863.

Nichol, Janet E. (1994): "A GIS-Based Approach to Microclimate Monitoring in Singapore's High-Rise Housing Estates." *Photogrammetric Engineering and Remote Sensing* 60(10):1225-32.

Pal, Swades, and Sk Ziaul. (2017): "Detection of Land Use and Land Cover Change and Land Surface Temperature in English Bazar Urban Centre." *Egyptian Journal of Remote Sensing and Space Science* 20(1):125-45. doi: 10.1016/j.ejrs.2016.11.003.

Rahaman, Saidur, Pankaj Kumar, Ruishan Chen, Michael E. Meadows, and R.B. Singh. (2020): "Remote Sensing Assessment of the Impact of Land Use and Land Cover Change on the Environment of Barddhaman District, West Bengal, India." *Frontiers in Environmental Science* 8(May 2021). doi: 10.3389/fenvs.2020.00127.

Samie, Abdus, Azhar Abbas, Muhammad Masood Azeem, Sidra Hamid, Muhammad Amjed Iqbal, Shaikh Shamim Hasan, and Xiangzheng Deng. (2020): "Examining the Impacts of Future Land Use/Land Cover Changes on Climate in Punjab Province, Pakistan: Implications for Environmental Sustainability and Economic Growth." *Environmental Science and Pollution Research* 27(20):25415-33. doi: 10.1007/s11356-020-08984-x.

Snyder, William C., Zhengming Wan, Yulin Zhang, and Y. Z. Feng. (1998): "Classification-Based Emissivity for Land Surface Temperature Measurement from Space." *International Journal of Remote Sensing* 19(14):2753-74.

Verburg, Peter H., Neville Crossman, Erle C. Ellis, Andreas Heinimann, Patrick Hostert, Ole Mertz, Harini Nagendra, Thomas Sikor, Karl Heinz Erb, Nancy Golubiewski, Ricardo Grau, Morgan Grove, Souleymane Konaté, Patrick Meyfroidt, Dawn C. Parker, Rinku Roy Chowdhury, Hideaki Shibata, Allison Thomson, and Lin Zhen. (2015): "Land System Science and Sustainable Development of the Earth System: A Global Land Project Perspective." *Anthropocene* 12:29-41. doi: 10.1016/j.ancene.2015.09.004.

Wang, Wenyin, Devendra Gauchan, A. Allan Degen, and Zhanhuan Shang. (2020): "Climate Change Mitigation and Pastoral Livelihood in the Hindu Kush Himalaya Region: Research Focuses, Opportunities and Challenges BT- Carbon Management for Promoting Local Livelihood in the Hindu Kush Himalayan (HKH) Region." Pp. 25-43 in, edited by Z. Shang, A.A. Degen, M.K. Rafiq, and V.R. Squires. Cham: Springer International Publishing.

Zewdie, Worku, and Elmar Csaplovics. (2015): "Remote Sensing Based Multi-Temporal Land Cover Classification and Change Detection in Northwestern Ethiopia." *European Journal of Remote Sensing* 48:121-39. doi: 10.5721/EuJRS20154808.